

# Feasibility study for the southern extension of Mila town (northeast of Algeria) for urbanization purposes: a geotechnical and hydrogeophysical approach

## *Studio di fattibilità per l'estensione meridionale della città di Misa (nord-est dell'Algeria) in previsione della sua urbanizzazione: approccio geotecnico e idrogeofisico*

Khoudir KHELLAF<sup>a</sup>, Mohamed Amine BECHKIT<sup>b</sup>, Wahid CHETTAH<sup>c</sup> ✉, El Hadj YUCEF BRAHIM<sup>d</sup>, Imane DIB<sup>e</sup>

<sup>a</sup>Laboratory of Valorization and Conservation of Arid Ecosystems, faculty of Sciences Nature and Life, Earth and Universe Sciences. University of Ghardaïa, Algeria - email: [kbellaf.khoudir@univ-ghardaia.dz](mailto:kbellaf.khoudir@univ-ghardaia.dz)

<sup>b</sup>Department of Geophysics. Houari Boumediene University of Sciences and Technology, Algiers, Algeria - email: [mohamed-amine.bechkit@botmail.fr](mailto:mohamed-amine.bechkit@botmail.fr)

<sup>c</sup>Laboratory of Geology and Environment, University of Constantine 1, Algeria - email ✉ : [wahid.chettah@umc.edu.dz](mailto:wahid.chettah@umc.edu.dz)

<sup>d</sup>Department of Earth Sciences, University of Batna 2, Algeria - email: [e.youcefbrahim@univ-batna2.dz](mailto:e.youcefbrahim@univ-batna2.dz)

<sup>e</sup>Laboratory of Applied Research in Engineering Geology, Geotechnics, Water Sciences, and Environment, Setif 1 University, Algeria email: [imane.dib@umc.edu.dz](mailto:imane.dib@umc.edu.dz)

### ARTICLE INFO

Ricevuto/Received: 24 January 2023

Accettato/Accepted: 7 April 2023

Pubblicato online/Published online:

30 June 2023

Handling Editor:

Silvia Bertoldo

### Citation:

Khellaf, K., Bechkit, MA., Chettah, W., Youcef Brahim EH., Dib, I. (2023). Feasibility study for the southern extension of Mila town (northeast of Algeria) for urbanization purposes: a geotechnical and hydrogeophysical approach. *Acque Sotteranee - Italian Journal of Groundwater*, 12(2), 49 - 64  
<https://doi.org/10.7343/as-2023-630>

### Correspondence to:

Wahid CHETTAH ✉  
[wahid.chettah@umc.edu.dz](mailto:wahid.chettah@umc.edu.dz)

**Keywords:** Algeria, geotechnics, hydrogeophysics, instability, Mila, soil, urbanization.

**Parole chiave:** Algeria, geotecnica, idrogeofisica, instabilità, Mila, terreno, urbanizzazione.

Copyright: © 2023 by the authors. License Associazione Acque Sotteranee. This is an open access article under the CC BY-NC-ND license: <http://creativecommons.org/licenses/by-nc-nd/4.0/>

### Riassunto

L'aumento della popolazione della città di Mila impone alle autorità competenti di estendere il centro abitato, ma l'instabilità dei terreni che caratterizzano la regione comporta la necessità di un approfondimento conoscitivo di dettaglio. In particolare, lo studio intende descrivere le caratteristiche geotecniche e geofisiche dei terreni di Marechau, area che rappresenta l'estensione sud-est della città. Per fornire una valutazione sullo stato dei terreni, scegliere il tipo di edificazione adeguato e in generale prendere decisioni ai fini costruttivi, è stato adottato un approccio di tipo geotecnico, caratterizzando i terreni mediante carotaggi, test penetrometrici e test di laboratorio. Sono state inoltre eseguite indagini geofisiche per determinare la resistività elettrica al fine di mappare la profondità del substrato roccioso. È stato effettuato anche un dettagliato studio idrogeologico, analizzando i dati di precipitazione e i livelli piezometrici del sistema acquifero per 200 giorni, e determinando la direzione dei deflussi sotterranei. I risultati dei sondaggi a carotaggio indicano un suolo argilloso con presenza di massi calcarei. Le prove penetrometriche dinamiche mostrano due tipologie di terreno distinte. I test di laboratorio rilevano che i materiali analizzati sono argillosi, molto plastici, sovraconsolidati, da medio a molto compressibili con potenziale di rigonfiamento da medio ad alto e media aggressività al calcestruzzo. Inoltre, i risultati della tomografia hanno evidenziato la presenza di un unico orizzonte stratigrafico (argilla) con massi incorporati. Il monitoraggio piezometrico ha individuato due acquiferi: uno superficiale e uno profondo in corrispondenza dei quali la ricarica non avviene istantaneamente a seguito di eventi di precipitazione e i deflussi sotterranei seguono la direzione del pendio. Tutti i risultati indicano che ai fini costruttivi è necessario valutare con attenzione soluzioni progettuali in relazione all'instabilità dei pendii: il quadro conoscitivo, ottenuto mediante la combinazione degli esiti sperimentali, la morfologia del terreno, l'assetto tettonico e gli aspetti sismotettonici, indica che l'area presenta un elevato rischio richiedendo necessariamente misure precauzionali rigorose.

### Abstract

The population of Mila is increasing and local authorities are looking for new lands to develop the town and provide housing. However, the soil of these lands is unstable and requires detailed studies to serve as a foundation. This work presents the geotechnical and the geophysical characteristics of the Marechau soils, which forms the southeast extension of the Mila town. To provide an idea about the soil condition, to choose the type of adequate constructions and to make decision for building it, we adopted a geotechnical approach, where we analysed the soils by carrying out core drilling tests, dynamic penetration tests and the laboratory tests. We also, employed the geophysical approach in determining the electrical resistivity so as to map the depth of bedrock roof. Furthermore, we conducted a comprehensive hydrogeological study, monitoring precipitation and the piezometric level of the aquifer over a period of 200 days, and determined the flow direction. The core drilling test results indicate a clayey soil with limestone blocks. The dynamic penetration test show two categories of soil. The laboratory tests show that the materials analysed are very plastic, over-consolidated and medium to very compressible. They have a medium to high swelling potential and medium amount of aggressiveness to concrete. Besides, the tomography results also showed a single layer land (clay) with massive rocks embedded in it. The piezometric monitoring reveals the presence of two aquifer systems. The first is superficial and the second is deep. They don't recharge directly after the rain falls and the groundwater flows in the direction of the slope. All the results indicate that solutions must be found for soil movements in the area under study before urbanization takes place. The combination of these results with the location, land morphology, tectonic activity, and seismotectonic aspects suggest that the area presents a high risk, and its urbanization requires rigorous and mandatory precautionary measures.

### Introduction

The Neogene Mila basin, to which our study area belongs (Marechau), is characterized by Upper-Miocene to Paleocene formations and is represented by the dominance of the lagoon-marine facies such as detritus deposits (conglomerates, gravels, sands, clays, marls, etc.), evaporative deposits (gypsum, anhydrites and rock salt, etc.), and lake limestones (Coiffait, 1992; Vila, 1980).

These deposits, especially clays, constitute the seat of many natural hazards: such as landslides, mass castings, swellings, settlements, etc. (Atmania, 2010; Tebbouche et al., 2022; Touati, 2019). These hazards result in significant damage to both public infrastructure and private properties; they distort the surface, disrupt roads, water and gas pipes, lead to cracks in buildings and houses etc. (Atmania, 2010; Benfedda et al., 2021; Khellaf, 2009; Khellaf et al., 2015; Khellaf & Hamimed, 2018 a,b; Labiod, 2009; Mutlutürk & Balcioglu, 2015). The best example of this situation is El Kherba area, which constitutes the future of Mila town extension towards the west side; it's one of the areas which threatened and affected by these land movements and already totally damaged (Benfedda et al., 2021; Tebbouche et al., 2022).

According to Azzouz (2015), Chen et al. (2019), Chettah (2009), Hadji et al. (2016), Khellaf (2019) and Khellaf & Hamimed (2018 c), these land movements are a result of heavy precipitation, variations in water content, hydrological and hydrogeological aspects, hydrostatic pressure caused by seasonal groundwater balances, as well as the influence of land slope, mineralogical composition of soil, seismic effects, and anthropogenic activities. These conditions impact the stability of foundations and lead to structural damage (Chanda et al., 2019; Khellaf, 2019; Tebbouche et al., 2022).

We conducted soil analyses of various geotechnical and hydrogeophysical parameters in order to comprehend phenomenon of their instability, as well as to determine the area's constructability in order to help in the resolution of the geological and geotechnical problems and to help find a new suitable land for urbanization.

### Material and methods

#### Location of the studied area and its characteristics

The field work showed that the studied area (Marechau) is characterized by 100 m thickness of limestone slab fractured resting on red clays. Both of these two formations belong to the Mio-Pliocene (Coiffait, 1992). This sector forms the southern extension of the Mila town to Marechau locality (about 7 km). It's bounded by Ain el Baidha on the north, Machta Ain el Kaf on the west, Bab Kassantina mound on the south, and Machta Ain Logna on the east (Fig. 1).

This area is in a predominantly hilly region. It's characterized by an average altitude of 500 m, sub-humid climate, little vegetal coverage limited at cereal crops with wild grasses and average annual precipitation of 588 mm/year (Aine el Bay rainfall station 2006).

The fieldwork observations indicate that the Marechau region has an irregular morphology marked by bulges, blisters etc. Their presence at the slope foot suggests that the region is prone to several natural hazards caused by the following factors:

1. The creep and solifluxion of the villafranchian red clays below the fractured limestone slab, facilitate the infiltration of the rainwater; which leads the saturation and crawling of these clays which leave this slab perched;
2. The blocks fall, which is due to the limestone slab predisposition, lead to detachment and the collapse of pieces and packages towards the north;

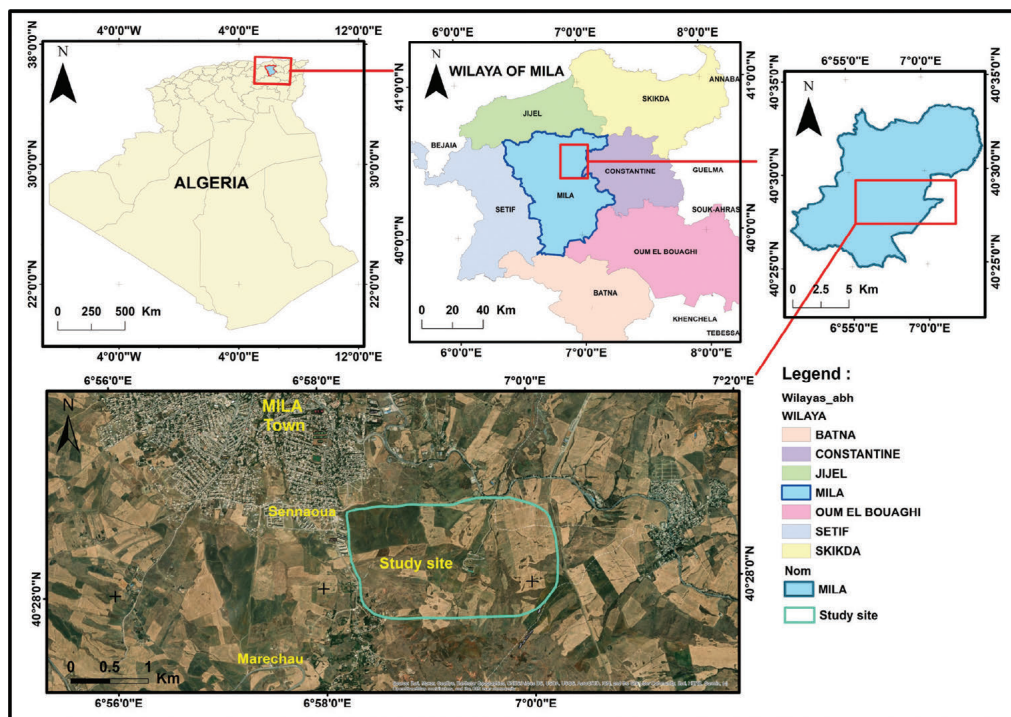


Fig. 1 - Location of the study area.

Fig. 1 - Ubicazione dell'area di studio.

3. The loose mass sliding (clays and limestone blocks) along the slope indicates the presence of several slides limited the downstream by bulges.

### Characteristics of the Mila region

#### Geological aspect

The geological works (Coiffait, 1992) carried out in the Mila region provided a litho-stratigraphic column, as shown below, which includes from bottom to top (Fig. 2):

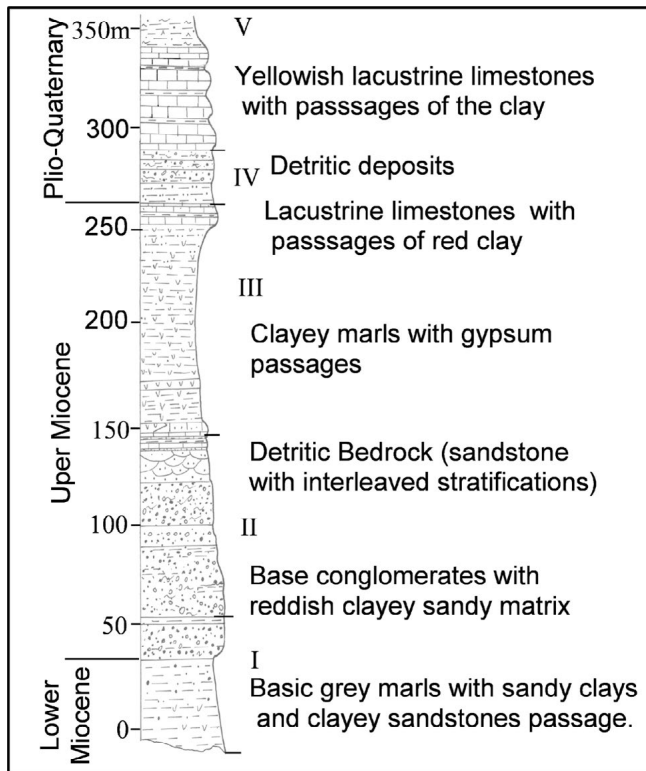


Fig. 2 - Lithostratigraphic column of the Mila basin Neogene deposits (Coiffait, 1992).  
Fig. 2 - Colonna stratigrafica dei depositi del bacino neogenico di Mila (Coiffait, 1992).

- I. Gray gypsum clays from the Mila river rest on tellian substratum. These basic clays are widely exposed around Mila town;
- II. Conglomerates with little rolled blocks, embedded in clay-sandy matrix and thin layer of sandstone with limestone cement (Durand-Delga, 1955). These conglomerate formations are reddish, 40 to 80 m thick, vallesian-lower turolian, are highly developed along of the Mila river;
- III. Marls which are mostly gray to black, but they can have reddish to purplish tints. These levels contain gypsum passages;
- IV. At the base of this unit, brownish gray marls sometimes yellowish brown, sandy, alternating with yellowish sandstone beds, and their thickness exceeding 20 m. These marls are surmounted by beige to yellowish sandstones alternating with clay-sandy layers. At their peaks, brown conglomerates with decimetric pebbles embedded in sand-pelitic matrix;

- V. A series constituted of very hard limestone slab, 50 to 100 m thick, whitish to reddish hue, and alternating with red clay levels.

#### Geomorphological aspect

The Mila region occupies a vast intermountain depression that extends from the Rhumel river to the north (200 m above sea level) and the Marechau hill to the south (1100 to 1200 m above sea level). Moreover, it's surrounded by very rugged reliefs with remarkable topographic contrasts (e.g. M'cid Aicha 1462 m above sea level) and the central part has low areas (Ouled el Kaïm depression) (Chettah, 2009; Khellaf, 2019).

The landscape of this region is characterized by an irregular morphology with a slope of 7 to 16%, occasionally exceeding 25% in certain areas (Chettah, 2009; Labiod, 2009), and by an important orographic aspect marked by very rugged elevations. These elevations are characterized by low hills with an average altitude of 500 meters (plains and valleys make up 55%, hills and foothills 30%, and mountains 15%), and they are intersected by a rather extensive network of rivers (Mebarki, 1984).

#### Tectonic aspect

Our study location is part of the Mila region, which has undergone many tectonic phases. According to Benabbas (2006) research, it has four main directional groups into which its effects are divided (Fig. 3):

1. The E-W (extensive): most of these accidents have a stall kinematics (dextral indentation);
2. The N-S: the majority of these accidents seem to present a delay appearance and sometimes are disturbed by other directional families, also it present sinisterly sliding movements;
3. The NE-SW: these accidents are well represented on the Mila central part and their extension would be regional;
4. The NW-SE: these accidents are visible at escarpments levels of limestone and sandstone massifs; its kinematics is being often dextral.

#### Seismicity

Several seismic studies conducted in the eastern Algeria show a relatively low to moderate seismic risk (Benfedda et al., 2017; Hamidatou & Sbatay, 2015; Maouche et al., 2011). Among these studies, we cite the Jijel earthquake 1856 (Harbi et al., 2011), Guelma earthquake 1937 (Benouar, 1994), the Constantine earthquake 1985 (Bounif et al., 1987), Beni Ilmane earthquake 2010 (Beldjoudi et al., 2016) etc. This region, in seismotectonic terms, is characterized by a complex neotectonic system comprising by an inverse fault and strike lateral shift right due to a NE-SW to E-W trending faults (Fig. 4) (Abbouda et al., 2019; Maouche et al., 2011), left lateral shift due to NW-SE trending faults (Abbes et al., 2015; Beldjoudi et al., 2016), and even normal faults located in Guelma basin (Aoudia et al., 2000). The active faults



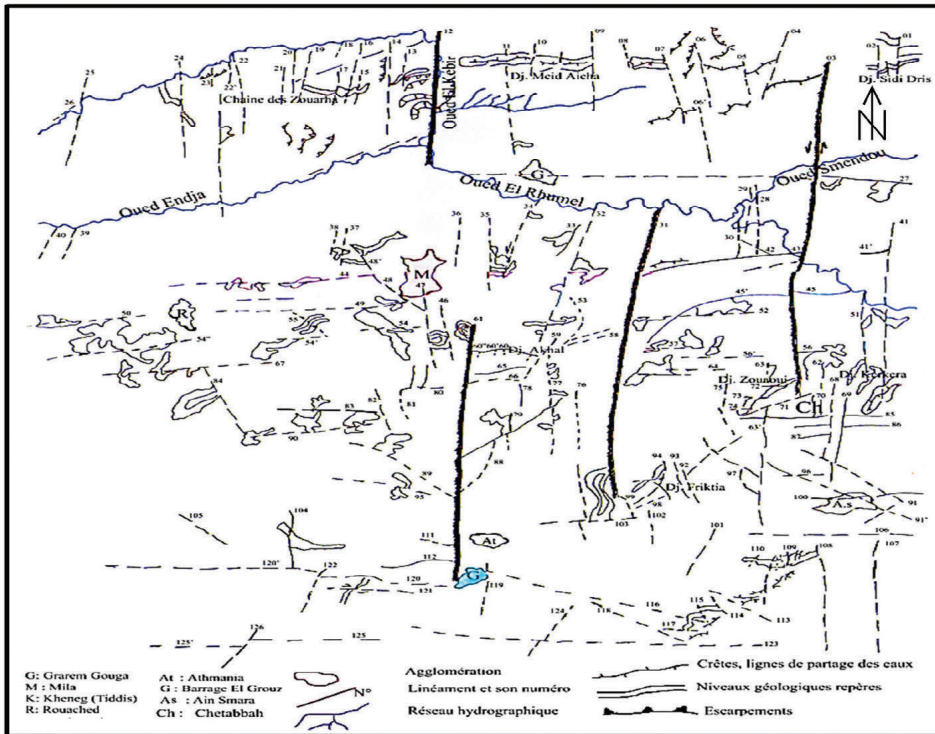


Fig. 3 - Tectonic interpretation map of the Mila basin with hydrographic network (Benabbas, 2006).

Fig. 3 - Mappa interpretativa dell'assetto tettonico del bacino di Mila con indicazione della rete idrografica (Benabbas, 2006).

have been described by Bouhadad (2008), Harbi et al.(1999), Meghraoui (1988), and Vila (1980); their potential has also been in the coastal areas such as Jijel, Annaba, and Skikda (Fig. 4) (Harbi et al., 2011; Kherroubi, 2009). The most recent earthquake affected the Mila region was on July 17<sup>th</sup>, 2020 (Mw = 4.6) at 8h12mn and on August 7<sup>th</sup>, 2020 (Mw = 4.8)

at 6h16mn and 11h13mn (Mw = 4.4). The last one, despite its relatively low magnitude, triggered extensive landslides in the centre area, caused huge damage, including the collapse of several structures, severe damage to dozens of others, and leaving hundreds of people homeless (Fig. 5) (Benfedda et al., 2021; Tebbouche et al., 2022).

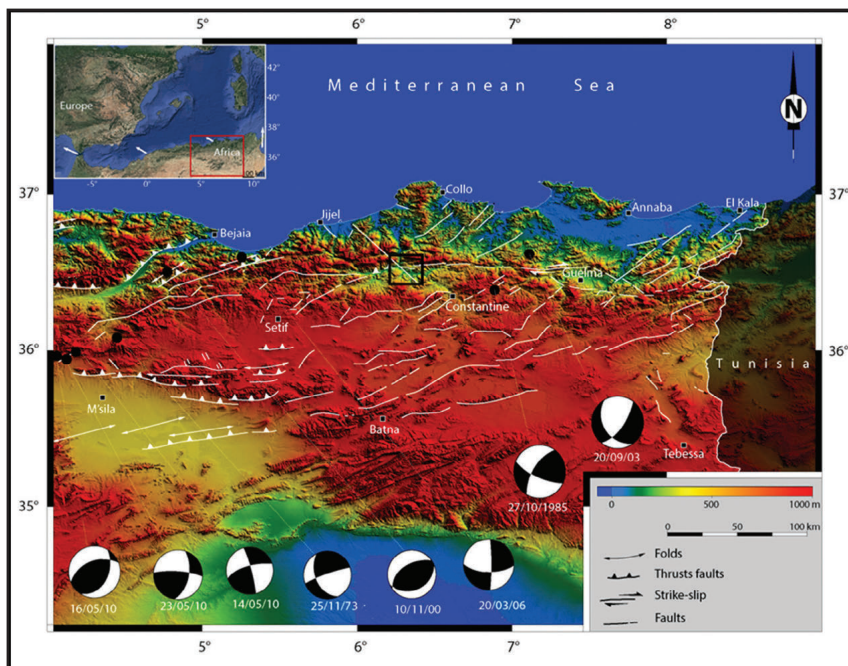


Fig. 4 - Map of seismotectonic framework for the eastern Algeria (Meghraoui, 1988). The black square: Mila region localization. The black and white circles: focal mechanism earthquakes (left to right, are: Mw=5.1, Mw=5.2, Mw=5.2, Ms=5.4, Mw=5.2, Ms=5.7 and Mb=4.8) (Ayadi & Bezzeghoud, 2015; Beldjoudi et al., 2016; Bouhadad et al., 2010; Bounif et al., 1987).

Fig. 4 - Carta sismotettonica dell'Algeria orientale (Meghraoui, 1988). Rettangolo nero: localizzazione della regione di Mila. Elementi grafici circolari bianchi e neri: meccanismi focali dei terremoti (da sinistra a destra: Mw=5.1, Mw=5.2, Mw=5.2, Ms=5.4, Mw=5.2, Ms=5.7 e Mb=4.8) (Ayadi & Bezzeghoud, 2015; Beldjoudi et al., 2016; Bouhadad et al., 2010; Bounif et al., 1987).

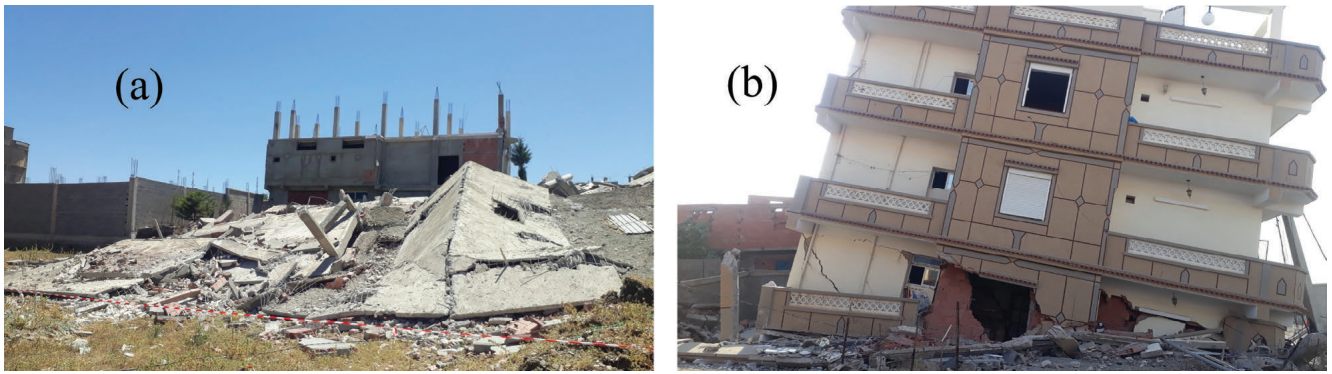


Fig. 5 - Catastrophic state of the Mila region houses after the August 7th, 2020 earthquake (a: Burial of the house with 5-stories, b: Burial of the ground floor and inclination of the rest).

Fig. 5 - Condizione catastrofica delle abitazioni nella regione di Mila dopo il terremoto del 07 agosto 2020 (a: cedimento di un edificio a 5 piani, b: cedimento del piano terra di un'abitazione e inclinazione del resto dell'edificio).

**Hydrological and hydrogeological aspect**

The Mila region belongs to the watershed basin of Kebir-Rhumel; it's characterized by heavy precipitation (588 mm). For this reason, it has a vast hydrographic network represented by the following rivers: Rhumel, El Kebir, El-Maleh and Mila. The prevalence of detritic deposits (conglomerates, gravel and sand) makes water storage and development of groundwater enhancement relatively favorable.

The area is intersected by several rivers which have a seasonal flow towards the north. The surface formations and the presence of limestone slab, fractured, and covers the slope, facilitates the rainwater infiltration to reaching the impermeable level (clays), which gives rise of several springs located at slab base offering an average flow to 13 L/s (Mebariki & Thomas, 1988).

**Methods**

A geotechnical investigation and soil reconnaissance program was conducted from February to March 2014. The program included over 20 core drillings test (S) at depths of 10 meters using the C400s retract sounding machine, more than 50 penetrometers test (P) at depths of 10 meters (with Borro B2 type), and a series of the laboratory tests (physico-mechanical and chemical tests using Triaxial press, frontal load Oedometer, Casagrande box etc.) on samples taken from various depths of the core borehole. Moreover, from October to December (dry season) and January to May (wet season), a piezometric monitoring was conducted. Figure 6 shows the position of these various investigation tests: the core drillings tests (S), the dynamic penetration tests (P), and the geo-electrical profiles (Ep) in the studied area.

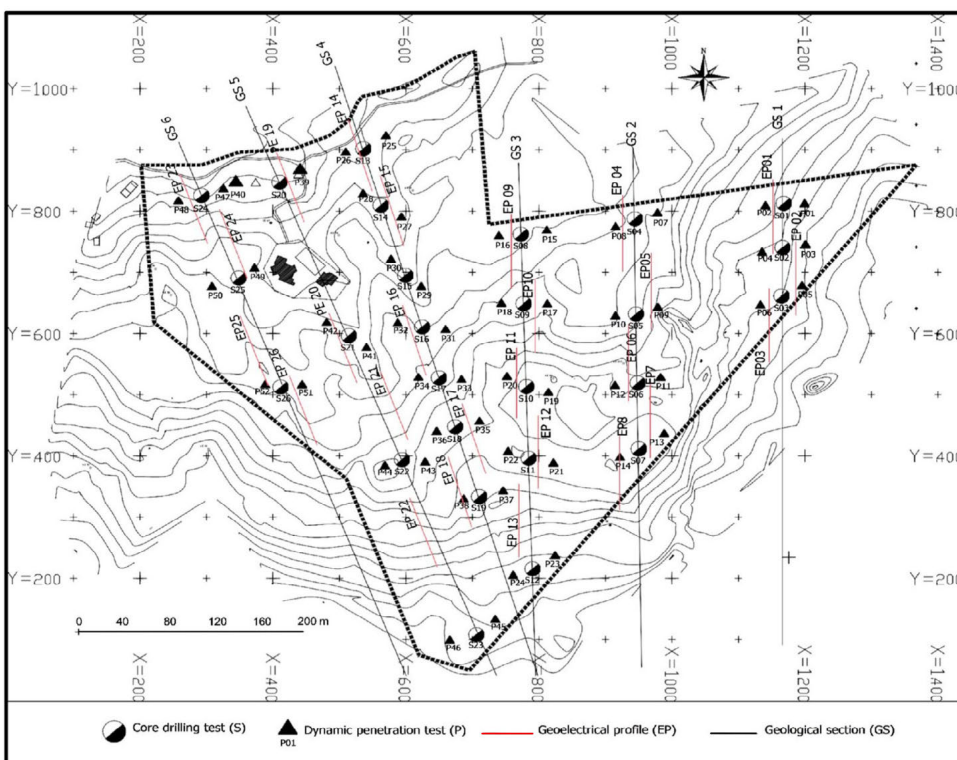


Fig. 6 - Location map of the core drillings tests (S), dynamic penetration tests (P) and geo-electrical profiles (Ep).

Fig. 6 - Ubicazione dei sondaggi a carotaggio (S), delle prove penetrometriche (P) e dei profili geoelettrici (Ep).



To determine the different layers succession in studying the vertical and the lateral geological formations variability, on the basis of their resistivity and thicknesses, more than 20 multi-electrode profiles (Ep) have been realised using the ABMN device (Wenner-Schlumberger type), moving along of line allowing for obtaining sections (2D). Each profile is made up of 24 electrodes spaced to 5 m apart. The apparent resistivity measurements can't be interpreted directly owing to the non-uniqueness of solution in heterogeneous land and their dependencies on the electrode configuration used (Parker, 1977); to obtain the true resistivity quantitative measurement, it's necessary to carry out a so-called inversion procedure. The processing of measurements inversion and their interpretation are carried out by high-performance software (Res2Dinv) (Loke, 1995).

In order to obtain the real resistivity of the soil in each point of the vertical section cross, the apparent resistivity values must be reversed, that is mean, to find a soil model (real resistivity) explaining the apparent measured resistivity (pseudo-section) to minimize the gap between the calculated and the measured pseudo-section for the soil model. This is quantified by Root Mean Square (RMS). The inversion process is described below: a starting model must be developed from the measured apparent resistivity data (A) and subsequently a model (C) is also developed either from the measured apparent resistivity data (A) or from prior information entered by the user. Then, the software (Res2Dinv) calculates the response of this model by performing "dummy acquisition",

the direct problem (i.e. the apparent resistivity calculation from true resistivity) being known (step 1) and thus the calculated profile (B) is obtained. Subsequently, the software determines the different degree (error) between the measured data (A) and the calculated profile (B) according to a certain criterion (step 2). The model is then modified to decrease the error between (A) and (B) (step 3). The operation must repeat iteratively until the error no longer decreases significantly (the process converges). Indeed, this model is modified with each iteration until the measured and the calculated data reach an acceptable match or until no further improvement is possible. In this case, the model is approximately close to the reality.

## Results and Discussions

### Geomorphology of the studied area within Mila region

The studied area is located at the Bab Kssantina mound foot. It has an irregular surface. This morphology suggests previous land movements that affected the area.

The area is characterized by the north slope. The slope map (Fig. 7) shows 5 classes: yellow indicates slopes with a gradient of less than 8% covering 26.39% of the studied area; green represents slopes with a gradient between 8 and 15% covering 23.18% of the area; blue indicates slopes with a gradient between 15 and 20% covering 21.70% of the area; orange represents slopes with a gradient between 20 and 35% covering 26.11% of the area, while red indicates slopes with a gradient more than 35% covering 2.63% of this area.

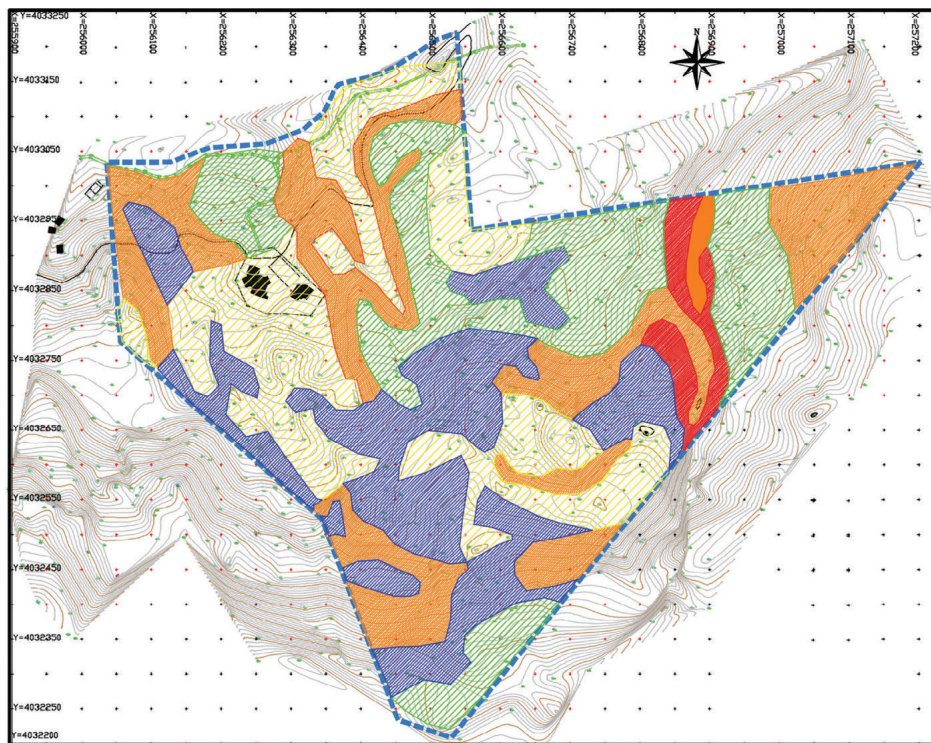


Fig. 7 - Slope Map of the studied area. The yellow color for the slope < 8%, the green color for the slope 8 to 15%, the blue color for the slope 15 to 20%, the orange color for the slope 20 to 35% and the red color for the slope > 35%.

Fig. 7 - Carta delle pendenze dell'area di indagine. In colore giallo la pendenza < 8%, in colore verde la pendenza compresa tra 8 e 15%, in colore blu la pendenza tra 15 e 20%, in colore arancio la pendenza tra 20 e 35% in colore rosso la pendenza > 35%.

**Geotechnical analyses**

**Core Drillings Test (S)**

The table below (Tab. 1) summarizes the lithological nature of the layers crossed in this area.

The lithological cross sections (Fig. 8) make it possible to know the soil lithology and its heterogeneous state, which composed of the brown silty clay (depth from 0 to 2.5 m) overlying the red clays with limestone blocks of different sizes (Tab. 1). These characteristics differ significantly from those observed in the same region located 1 kilometer to the west, where gray to greenish altered marl, gray clays, and topsoil are present. (Khellaf, 2019; Khellaf & Hamimed, 2018a).

Suiki (2007) shows that the clay deposits, across Mila basin, contain fine intercalations of gypsum, conglomerate levels and lake limestones. This succession indicates that this basin is a large lagoon for lagoon-continental deposits of mio-pliocene with a remarkable fluctuation of sea level which is associated to the tectonic and paleoclimate influence.

Tab. 1 - Lithological characteristics of the Marechau area.

Tab. 1 - Caratteristiche litologiche dell'area di Marechau.

|                                       | Depth (m) | Lithology                       |
|---------------------------------------|-----------|---------------------------------|
| <b>Geological cross section (GS3)</b> |           |                                 |
| S8                                    | 0 to 1.2  | Brown silty clay                |
|                                       | 1.2 to 10 | Red clays with limestone blocks |
| S9                                    | 0 to 1.2  | Brown silty clay                |
|                                       | 1.2 to 10 | Red clays with limestone blocks |
| S10                                   | 0 to 1.2  | Brown silty clay                |
|                                       | 1.2 to 10 | Red clays with limestone blocks |
| S11                                   | 0 to 2.2  | Brown silty clay                |
|                                       | 2.2 to 10 | Red clays with limestone blocks |
| S12                                   | 0 to 1.2  | Brown silty clay                |
|                                       | 1.2 to 10 | Red clays with limestone blocks |
| <b>Geological cross section (GS4)</b> |           |                                 |
| S13                                   | 0 to 1.2  | Brown silty clay                |
|                                       | 1.2 to 10 | Red clays with limestone blocks |
| S14                                   | 0 to 10   | Red clays with limestone blocks |
| S15                                   | 0 to 10   | Red clays with limestone blocks |
| S16                                   | 0 to 10   | Red clays with limestone blocks |
| S17                                   | 0 to 1.2  | Brown silty clay                |
|                                       | 1.2 to 10 | Red clays with limestone blocks |
| S18                                   | 0 to 1.2  | Brown silty clay                |
|                                       | 1.2 to 10 | Red clays with limestone blocks |
| S19                                   | 0 to 1.2  | Brown silty clay                |
|                                       | 1.2 to 10 | Red clays with limestone blocks |
| S20                                   | 0 to 10   | Red clays with limestone blocks |
| <b>Geological cross section (GS5)</b> |           |                                 |
| S21                                   | 0 to 10   | Red clays with limestone blocks |
| S22                                   | 0 to 10   | Red clays with limestone blocks |
| S23                                   | 0 to 10   | Red clays with limestone blocks |

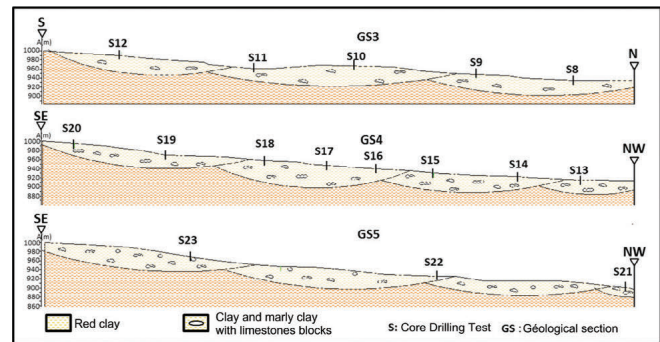


Fig. 8 - Lithological cross sections of the Marechau area.

Fig. 8 - Sezioni litologiche dell'area di Marechau.

**Dynamic Penetration Tests (P)**

The obtained results from these tests are both represented in the Table 2.

The analysis of these results leads to the results described below.

The bedrock is recorded at depths from 1.2 to 4.8 m, except for P8 and P16 it is found at a depth of 0.8 m (Tab. 2). These characteristics are different from those we found in the same region (1 km on to the west), where we encountered it at 1.6 to 9.6 m deep (Khellaf, 2019; Khellaf & Hamimed, 2018b) and on the El Kherba region from 1.6 to 10 m made by LNHC in 2001 and Aiche-Géo-Sol laboratory in 2013.

The penetrometer curves of all tests carried out in the Marechau sector field indicate a minimum peak resistance ( $Pr_{min}$ ) of 50 to 100 bars except in P4, P8, P12, P19, and P25 which show higher values (over 115 bars) (Tab. 2), but in El Kherba region we encountered the  $Pr_{min}$  are from 30 to 95 bars and 20 to 50 bars.

The maximum peak resistance ( $Pr_{max}$ ) is varied from 145 to 250 bars for all tests (Tab. 2), which is different from those we found in the El Kherba region (from 200 to 500 bars and 220 to 650 bars).

According to Géoxplo (2015), Khellaf (2019), Khellaf & Hamimed (2018 c) and LBM-Sol (2014) works, the variation of these results is due to the presence of limestone blocks, enveloped in the clay matrix that sometimes stop the advancement of drilling tools (Zouaoui, 2008) and distort the results ( $Pr_{min}$  reaches 150 bars and  $Pr_{max}$  exceeds 400 bars). Moreover, the presence of water increases the soil saturation degree and subsequently makes it loose (LBM-Sol, 2014).

These results can help us to define two categories of soil in the studied area: the first has a high peak resistance ( $Pr_{min} > 115$  bars,  $Pr_{max}$  reaches 250 bars) and bedrocks at 4.8 m of depth, and the second present an average peak resistance value ( $145 < Pr_{max} < 250$  bars,  $55 < Pr_{min} < 80$  bars) and bedrocks over 1.2 m.

Therefore, it is essential to consider the impact of these parameters when calculating settlements in order to make informed decisions about urban development.

Tab. 2 - Penetrometer characteristics of the Marechau region soils.

Tab. 2 - Caratteristiche dei terreni della regione di Marechau edotte dalla indagini penetrometriche.

| Penetrometer (P) | Bed Rocks BR (m) | Minimum peak resistance (bars) | Maximum peak resistance (bars) | Penetrometer (P) | Bed Rocks BR (m) | Minimum peak resistance (bars) | Maximum peak resistance (bars) |
|------------------|------------------|--------------------------------|--------------------------------|------------------|------------------|--------------------------------|--------------------------------|
| P1               | 1.2              | 50                             | 200                            | P27              | 3.6              | 90                             | 160                            |
| P2               | 1.2              | 60                             | 200                            | P28              | 3.2              | 48                             | 165                            |
| P3               | 2.2              | 80                             | 200                            | P29              | 2.8              | 48                             | 180                            |
| P4               | 1.8              | 115                            | 200                            | P30              | 2.6              | 50                             | 180                            |
| P5               | 1.2              | 80                             | 200                            | P31              | 4.2              | 45                             | 150                            |
| P6               | 2.0              | 100                            | 180                            | P32              | 4.0              | 60                             | 155                            |
| P7               | 2.4              | 80                             | 155                            | P33              | 4.8              | 90                             | 145                            |
| P8               | 0.8              | 110                            | 250                            | P34              | 3.8              | 50                             | 155                            |
| P9               | 1.4              | 80                             | 200                            | P35              | 3.2              | 60                             | 150                            |
| P10              | 1.6              | 80                             | 200                            | P36              | 2.8              | 60                             | 190                            |
| P11              | 2.2              | 80                             | 200                            | P37              | 3.4              | 70                             | 250                            |
| P12              | 2.6              | 115                            | 170                            | P38              | 2.8              | 55                             | 250                            |
| P13              | 3.2              | 80                             | 165                            | P39              | 2.8              | 55                             | 170                            |
| P14              | 2.8              | 75                             | 170                            | P40              | 3.0              | 70                             | 170                            |
| P15              | 3.4              | 80                             | 160                            | P41              | 1.6              | 80                             | 250                            |
| P16              | 0.8              | 50                             | 250                            | P42              | 2.0              | 80                             | 200                            |
| P17              | 3.2              | 100                            | 200                            | P43              | 4.0              | 55                             | 250                            |
| P18              | 2.4              | 80                             | 250                            | P44              | 4.4              | 55                             | 145                            |
| P19              | 2.4              | 120                            | 200                            | P45              | 3.8              | 80                             | 250                            |
| P20              | 2.0              | 100                            | 190                            | P46              | 4.0              | 70                             | 250                            |
| P21              | 3.0              | 80                             | 170                            | P47              | 2.2              | 55                             | 200                            |
| P22              | 3.2              | 55                             | 170                            | P48              | 1.8              | 80                             | 250                            |
| P23              | 3.4              | 50                             | 200                            | P49              | 4.4              | 52                             | 250                            |
| P24              | 2.8              | 48                             | 200                            | P50              | 4.8              | 60                             | 150                            |
| P25              | 4.2              | 120                            | 160                            | P51              | 3.0              | 56                             | 155                            |
| P26              | 3.2              | 55                             | 160                            | P52              | 2.6              | 65                             | 170                            |

Tab. 3 - Physico-mechanical characteristics of examined soils.

Tab. 3 - Caratteristiche fisico-meccaniche dei terreni esaminati.

|                           |                                 |           |           |           |           |           |           |           |           |           |           |           |           |           |           |
|---------------------------|---------------------------------|-----------|-----------|-----------|-----------|-----------|-----------|-----------|-----------|-----------|-----------|-----------|-----------|-----------|-----------|
| Chemical analyzes         | SO <sub>4</sub> 2H <sub>2</sub> | 4.70      | 5.42      | 6.91      | 5.96      | 4.61      | 5.04      | 5.24      | 5.81      | 8.05      | 7.81      | 5.51      | 6.60      | 5.97      | 4.90      |
|                           | CaCO <sub>3</sub>               | 10.00     | 15.00     | 10.00     | 15.55     | 22.10     | 20.05     | 25.00     | 28.77     | 18.67     | 15.00     | 14.25     | 10.36     | 10.00     | 10.00     |
| Shear straight            | Φ <sub>uu</sub> (°)             | 3.80      | 3.37      | 5.37      | 3.74      | 1.26      | 4.30      | 3.09      | 3.37      | 5.20      | 3.83      | 4.67      | 2.03      | 3.97      | 3.98      |
|                           | C <sub>uu</sub> (bars)          | 0.75      | 0.79      | 0.71      | 0.77      | 0.83      | 0.76      | 0.79      | 0.84      | 0.74      | 0.77      | 0.75      | 0.79      | 0.69      | 0.76      |
| Oedometer Compressibility | C <sub>g</sub> (%)              | 2.54      | 2.74      | 2.73      | 2.56      | 3.97      | 3.41      | 3.09      | 3.24      | 3.76      | 2.64      | 3.29      | 2.95      | 3.11      | 3.55      |
|                           | C <sub>c</sub> (%)              | 16.28     | 15.95     | 13.95     | 13.90     | 12.29     | 15.61     | 22.92     | 14.62     | 15.95     | 16.94     | 11.63     | 12.96     | 11.29     | 12.29     |
|                           | P <sub>c</sub>                  | 3.42      | 3.50      | 2.56      | 2.98      | 2.90      | 3.15      | 3.02      | 2.76      | 2.18      | 3.59      | 2.15      | 2.49      | 2.18      | 2.54      |
| Atterberg Limites         | I <sub>p</sub> (%)              | 25.74     | 30.68     | 28.95     | 28.98     | 30.74     | 30.34     | 30.74     | 29.61     | 31.56     | 28.52     | 29.98     | 27.86     | 24.88     | 29.94     |
|                           | WL (%)                          | 54.09     | 58.66     | 54.37     | 59.45     | 58.12     | 57.09     | 58.12     | 59.47     | 61.03     | 58.97     | 52.00     | 54.57     | 48.75     | 57.48     |
| Granularity               | 2μm                             | 56        | 54        | 48        | 38        | 58        | 50        | 56        | 88        | 74        | 74        | 86        | 86        | 86        | 80        |
|                           | 80μm                            | 92        | 89        | 90        | 82        | 98        | 86        | 94        | 44        | 82        | 86        | 92        | 95        | 94        | 87        |
|                           | 2mm                             | 95        | 97        | 99        | 90        | 100       | 97        | 100       | 100       | 92        | 99        | 100       | 100       | 100       | 96        |
| Sr (%)                    |                                 | 98.40     | 95.68     | 99.74     | 100       | 100       | 94.78     | 94.66     | 100       | 100       | 98.52     | 100       | 100       | 95.74     | 99.57     |
| ds (t/m <sup>3</sup> )    |                                 | 1.60      | 1.63      | 1.59      | 1.61      | 1.59      | 1.65      | 1.60      | 1.58      | 1.54      | 1.58      | 1.67      | 1.60      | 1.71      | 1.69      |
| W (%)                     |                                 | 25.24     | 22.51     | 26.55     | 25.33     | 25.94     | 22.45     | 24.06     | 26.76     | 28.47     | 25.41     | 22.75     | 25.88     | 21.74     | 23.87     |
| D (m)                     |                                 | 2.80-3.50 | 4.20-5.20 | 1.50-2.00 | 3.20-4.00 | 1.20-2.20 | 3.00-3.50 | 1.20-2.20 | 2.50-3.00 | 1.20-2.20 | 2.50-3.00 | 1.20-2.00 | 3.60-4.10 | 1.20-1.90 | 2.50-3.00 |
|                           |                                 | S1        |           | S2        |           | S4        |           | S5        |           | S7        |           | S8        |           | S10       |           |



**Laboratory tests**

The obtained results are grouped in the Table 3. These tests gave:

- a. The water content (w) from 20.49 to 30.02%, the dry density (ds) from 1.54 to 1.75 t/m<sup>3</sup> and the saturation degree (Sr) from 91.35 to 100%. So, the soil examined is moderately humid, saturate (Cordary, 1994; NF P94-050; Philipponnat, 1979; Philipponnat & Hubert, 2003) and dense (Costet & Sanglerat, 1981; NF P94-053). In Azouz (2015), Chettah (2009), Géoexplo (2015), Khellaf (2019), Khellaf & Bitat (2006) works it is shown that these characteristics are the triggering factors for land movements. Also, Khellaf & Hamimed (2018a) show that these clays are characterized by the abundance of minerals which have volume variation at water presence, such as vermiculite, chlorite, montmorillonite, etc. These minerals, despite their low concentrations, are involved in the generation of land movements.
- b. The liquidity limits (WL) from 48.6 to 62.75%, the plasticity limits (PL) from 21.23 to 32.30%, the plasticity index (Ip) from 24.88 to 31.56% and the consistency index (Ic) from 0.71 to 1.19%. According to the fine soil classifications on the Casagrande diagram, the materials examined are very plastic and consistent clays. They present a large difference between the natural water content and the liquidity limits which demonstrates high over-consolidation state and desiccation of soil (Derriche and al., 1999). According to Dakshanamurthy & Raman (1973), Hazmoune (2008), Khellaf & Hamimed, (2018 b) and Komornik & David (1969) works, these results reveal the increase of consistency index values (> 1.5), dry density which is greater than 1.5 t/m<sup>3</sup> and the Atterberg

limit values that are higher than standards. So, the studied clays are swelling.

- c. The particle size and the sedimentometric analyses gave the sand content of 11.50%, silt about 29% and clay percentage of 59.50%. According to the NF P94-057, the soil identification triangle, Philipponnat (1979) also Costet & Sanglerat (1981), the studied soil is clays and silty clays which classified in category "I".
- d. For depth of 1.20 to 6 m, the soil presents cohesion (C<sub>UU</sub>) from 0.67 to 0.84 bars, low internal friction angle (φ<sub>UU</sub>) which from 2.25 to 5.20°, pre-consolidation stress (Pc) varies from 1.17 to 3.81 bars, compressibility index (Cc) varies from 10.96 to 23.59% and swelling index (Cs) varies from 2.57 to 4.48%. The classification of soils according Costet & Sanglerat (1981) indicates that this facies are clay. These clays are consistent, over-consolidated, medium to very compressible and medium to high swelling potential (Mutlutürk & Balcioğlu, 2015; NF P94-090-1; Philipponnat, 1979). Also, the Zouaoui (2008) works show that the increase of the water content systematically leads the reduction of the characteristics such as the internal friction angle (φ), the cohesion (C) (undrained), the shear strength etc., where Alijani-Shirvani & Shooshpasha (2015), confirm that the water content (w) leads it's softening, which means the progressive increase in its deformability under load.
- e. The chemical analyses gave the sulphate and 10 to 30.5% of carbonate (CaCO<sub>3</sub>) (Tab. 3). These results indicate a medium aggressiveness on concrete for the majority of surfaces (NF P18-011) and average calcium carbonate contents (<30%) which is a good mechanical resistance index of this soil (Cordary, 1994). So, the Marechau

Tab. 3 - Physico-mechanical characteristics of examined soils.

Tab. 3 - Caratteristiche fisico-meccaniche dei terreni esaminati.

|           |           |           |           |           |           |           |           |           |           |           |           |           |           |           |           |           |           |           |           |
|-----------|-----------|-----------|-----------|-----------|-----------|-----------|-----------|-----------|-----------|-----------|-----------|-----------|-----------|-----------|-----------|-----------|-----------|-----------|-----------|
| 10.00     | 15.52     | 12.28     | 15.55     | 5.04      | 5.95      | 6.05      | 7.01      | 4.86      | 6.60      | 6.27      | 7.50      | 5.04      | 5.74      | 8.81      | 7.04      | 6.10      | 5.11      | 8.64      | 4.63      |
| 91.74     | 86.95     | 87.65     | 83.05     | 10.00     | 15.55     | 15.00     | 18.65     | 12.20     | 15.02     | 20.50     | 25.00     | 28.30     | 28.55     | 30.05     | 30.15     | 28.30     | 19.85     | 30.05     | 19.55     |
| 0.75      | 0.77      | 0.72      | 0.74      | 4.52      | 4.16      | 5.28      | 3.18      | 3.98      | 3.58      | 4.23      | 2.27      | 5.68      | 3.40      | 3.54      | 3.75      | 5.48      | 3.58      | 5.45      | 2.85      |
| 2.96      | 3.08      | 2.53      | 3.35      | 0.72      | 0.75      | 0.69      | 0.79      | 0.76      | 0.76      | 0.71      | 0.83      | 0.73      | 0.77      | 0.79      | 0.73      | 0.74      | 0.76      | 0.67      | 0.80      |
| 14.28     | 14.62     | 8.64      | 14.95     | 3.06      | 3.99      | 3.28      | 4.48      | 3.80      | 3.18      | 2.57      | 3.13      | 2.76      | 3.27      | 2.23      | 3.24      | 3.79      | 2.97      | 2.54      | 2.84      |
| 1.79      | 2.05      | 1.17      | 2.86      | 10.30     | 15.61     | 11.63     | 22.26     | 20.93     | 15.61     | 16.94     | 17.27     | 16.28     | 17.61     | 10.96     | 16.28     | 20.93     | 22.92     | 13.29     | 22.92     |
| 28.85     | 29.44     | 28.43     | 28.95     | 1.93      | 2.05      | 1.73      | 2.90      | 2.24      | 3.07      | 3.16      | 3.81      | 3.23      | 3.65      | 2.05      | 3.28      | 2.73      | 3.02      | 2.91      | 3.30      |
| 30.12     | 26.89     | 30.28     | 25.96     | 33.55     | 31.13     | 30.00     | 28.30     | 28.67     | 25.68     | 27.67     | 27.12     | 28.59     | 26.43     | 26.27     | 28.07     | 27.22     | 28.36     | 25.53     | 31.27     |
| 47        | 54        | 54        | 55        | 61.23     | 57.91     | 62.57     | 54.67     | 52.35     | 51.05     | 48.90     | 51.47     | 49.93     | 51.28     | 50.38     | 53.94     | 48.67     | 52.13     | 50.87     | 58.16     |
| 78        | 82        | 80        | 86        | 56        | 44        | 46        | 56        | 57        | 58        | 50        | 47        | 46        | 56        | 50        | 49        | 52        | 56        | 45        | 51        |
| 88        | 90        | 87        | 94        | 89        | 83        | 85        | 94        | 91        | 93        | 85        | 82        | 80        | 91        | 83        | 85        | 83        | 90        | 79        | 90        |
| 95        | 97        | 95        | 100       | 99        | 94        | 98        | 100       | 95        | 100       | 93        | 96        | 91        | 98        | 93        | 100       | 95        | 96        | 93        | 100       |
| 96.25     | 92.04     | 100       | 97.54     | 100       | 98.69     | 100       | 95.68     | 95.34     | 91.78     | 91.35     | 100       | 100       | 100       | 96.87     | 100       | 95.76     | 92.68     | 100       | 93.87     |
| 1.58      | 1.70      | 1.53      | 1.65      | 1.57      | 1.59      | 1.56      | 1.63      | 1.58      | 1.75      | 1.68      | 1.59      | 1.75      | 1.54      | 1.71      | 1.69      | 1.73      | 1.70      | 1.73      | 1.68      |
| 26.87     | 20.87     | 27.58     | 26.31     | 28.96     | 26.37     | 29.78     | 24.78     | 26.99     | 20.44     | 20.49     | 25.94     | 20.70     | 29.02     | 22.47     | 25.12     | 21.78     | 22.86     | 20.78     | 23.67     |
| 1.20-2.20 | 2.50-3.00 | 1.20-2.00 | 3.50-4.00 | 1.20-2.00 | 3.00-3.70 | 1.50-2.00 | 2.60-3.00 | 1.50-2.00 | 4.10-5.00 | 1.30-2.30 | 2.60-3.20 | 2.80-3.80 | 5.10-6.00 | 2.50-3.10 | 4.00-4.50 | 1.20-1.80 | 2.50-3.00 | 1.50-2.50 | 3.50-4.20 |
| S12       | S13       | S16       | S17       | S18       | S21       | S22       | S23       | S24       | S26       |           |           |           |           |           |           |           |           |           |           |

clayey formations contain sulphates (Aiche-Géo-Sol, 2013; Géoxplo, 2015; LBM-Sol, 2014), which come from the dissolution of the interstratified gypsum formation within these clays (El Yakoubi, 2006; Khellaf, 2019; Khellaf & Hamimed, 2018b; Rollingset al., 1999).

### **Geophysical analyses (Electrical resistivity)**

The results are summarized in the geo-electrical profiles (EP) shown in Figure 9, which indicate the soil in the studied area is composed from top to bottom of:

- a. Brown silty clay with low resistivity range (10 to 50 ohm-m);
- b. Red clays with limestone blocks and their resistivity can reach 1000 ohm-m;
- c. Marly clays with an intermediate resistivity (50 to 100 ohm-m).

The thickness of these layers varies from one geo-electrical profile to another (Fig. 9). Mostly, the limestone rocks are shown in the geo-electrical profiles Ep1, Ep2, Ep4, Ep9, Ep14, and Ep16. In the other cases (in the profiles Ep6, Ep11, Ep13, Ep15, Ep17, Ep18, Ep22, and Ep26), these limestone rocks are found near the ground surface with a metric thickness (average of 10 m) and a variable extent that can occupy the geo-electrical profile size (115 m) (e.g. Ep4). Usually, they exhibit resistivity values of 300 ohm-m, but these values can reach 1000 ohm-m at Ep6, Ep9, Ep11, Ep16, and Ep26. Also, we mark the absence of them, or they were completely replaced by silty clay for a distance equal to the half of geo-electrical profiles size, in the Ep9, Ep11 and Ep13.

The error is represented by the difference between pseudo-section calculated for soil model and pseudo-section measured (quantified by RMS), and it varies between 1.7% (in Ep3) and 7.8% (in Ep9) which remains acceptable.

Indeed, the analysis of the geo-electrical imaging profiles allowed us to infer the presence of three models:

1. The Ep9, Ep11, and Ep13 exhibit lateral heterogeneity – model (a) - with a rapid passage of clays to heterogeneous soils containing limestone blocks. This part of soil presents more or less resistant characteristics and an average of 15 m thickness, but the superficial and the depth resistivity still become very low due to the presence of clay. In reality, there are limestone blocks embedded in a clay matrix. As a result, the zone of rapid lateral transition (clay - limestone blocks), can be considered as an axis for landslides which favors more rainwater infiltrations and gives rise to shear movements.
2. In contrast, the Ep1, Ep2, Ep4, Ep6, Ep14, Ep15, Ep16, Ep17, Ep18 and Ep22 show a model (b) with three layers: the first is superficial, conductor, porous, silt-clay layer favoring the water circulation in the soil, and it has low resistivity (10 to 50 ohm-m). The last is marl-clay layer characterized by an intermediate resistivity (50 to 100 ohm-m). Between the two, we note the presence of limestone block layers, shallow, consolidated, and resistant. Indeed, these layers have an increasing resistivity (reaches 1000 ohm-m); their thickness can be,

in some places, from 15 to 20 m, and it can probably be considered as possible foundations substratum. So, the first instability zone (porous silt-clay) is shallow and superficial, separating from the second composed of limestone blocks. To this, we added marly-clay masses which can play, again, the sliding factor role for greater magnitude. According to the Mebarki (1984) and Géoxplo work in 2015, this region is characterized by the presence of several springs near landslide fronts which constitute a catalyst factor to accentuate the magnitude and also the movements triggered speed. These factors would make this region more and more vulnerable to the soil and subsoil recurrent instabilities.

3. For the Ep26, we have the predominant of model (c) with two layers. The first is based on the limestone blocks which are located close in the ground surface. This layer rests on the second which is the marly-clay nature. From there, the presence of water in studied area, which separates the surface layer from the deeper, favoring the presence of landslide. In the geomechanical point of view, the association of clays with water favours its adsorption and absorption, hence a certain significant swelling capacity given their specific surface which can generate surface sliding.

Therefore, the geophysical prospection revealed that the studied area is composed by a clay layer that envelops the limestone blocks and contains water which makes the decline of soil characteristics (water content, resistivity etc.) and generate the landslides. These conditions are unfavorable for the urbanization of this area.

### **Hydrogeological behavior of the aquifer system in Mila region**

The monitoring results of the aquifer system behavior and the groundwater flow direction in the Mila region (north of the studied area) over a period of 200 days (from October 2013 to May 2014) are summarized in Fig. 10, Fig. 11, Fig. 12 and Fig. 13.

During the 200-day period, variations in the levels of some core drillings (CD) wells that were 20 meters deep (Fig. 10) were monitored. The curves show a variation of -0.95 to -2.55 meters in CD1, -1.3 to -1.8 meters in CD2 and -2 to -2.8 meters in CD3. Additionally, some piezometers (P) were installed at depths exceeding -50 meters and monitored; they show a variation of -0.5 to -0.8 meters in P2, P4, and P7, -5 to -7.4 meters in P5, and -8 to -10 meters in P6, while P1 (-0.8 meters) and P3 (-1.4 meters) maintained a constant level. The precipitation recorded during this period was significant (Fig. 11): we measured a rate ranging from 70 to 175 mm for the first 30 days (autumn) and from 55 to 210 mm for the 170 days (winter and spring). The geological formations that make up this area have a permeability, measured for depths up to 18 m and under different constraints, which varies from  $1.21 \cdot 10^{-7}$  to  $6.01 \cdot 10^{-7}$  cm/s,  $1.97 \cdot 10^{-7}$  to  $5.52 \cdot 10^{-7}$  cm/s,  $1.44 \cdot 10^{-7}$  to  $5.53 \cdot 10^{-7}$  cm/s, and  $1.19 \cdot 10^{-7}$  to  $3.46 \cdot 10^{-7}$  cm/s for depths of 2.3 to 3 m, 4.1 to 4.8 m, 11 to 11.5 m, and 17 to 18 m and for pressure of consolidation (PC) of 1.3 bars,

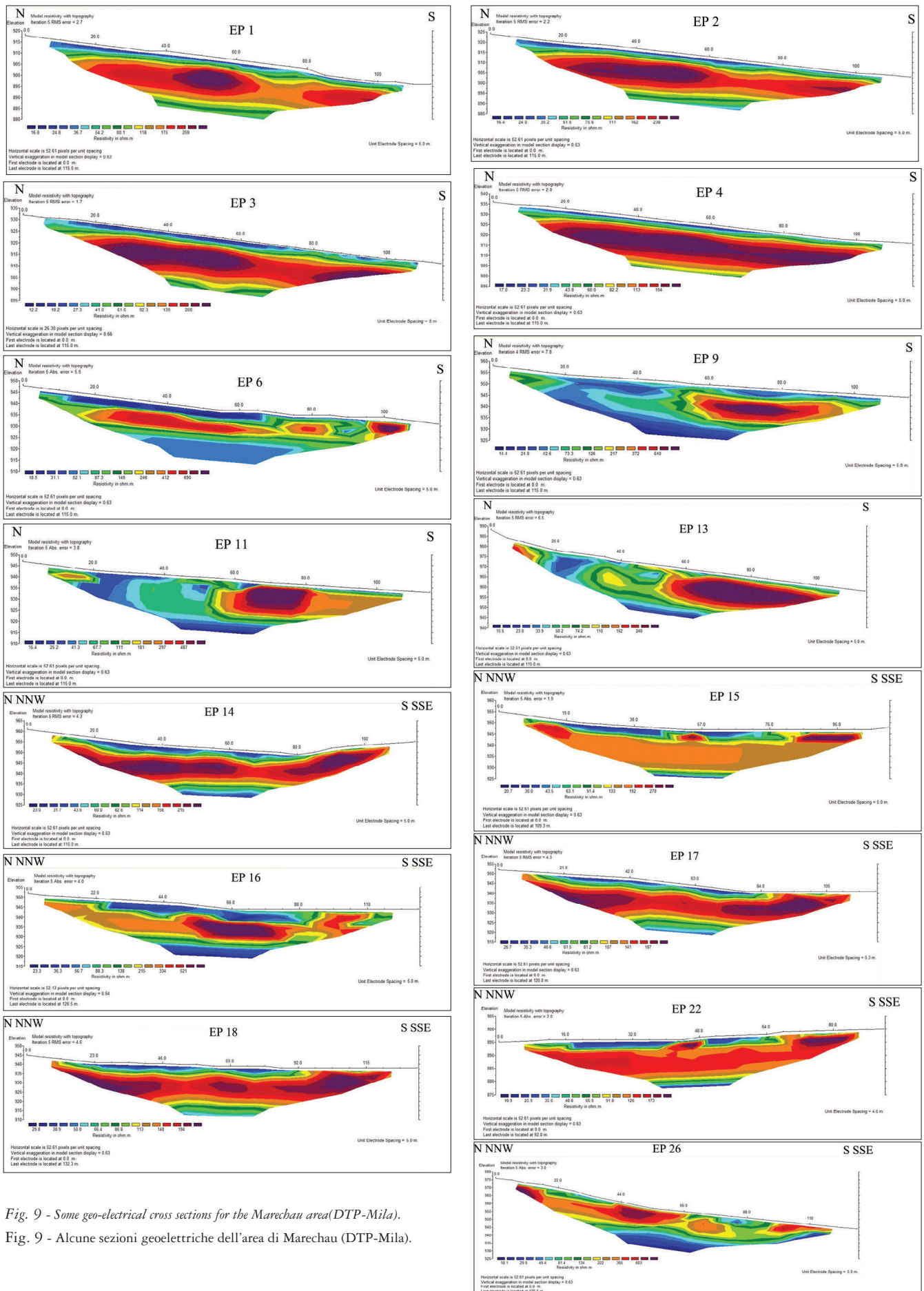


Fig. 9 - Some geo-electrical cross sections for the Marechau area(DTP-Mila).

Fig. 9 - Alcune sezioni geoelettriche dell'area di Marechau (DTP-Mila).



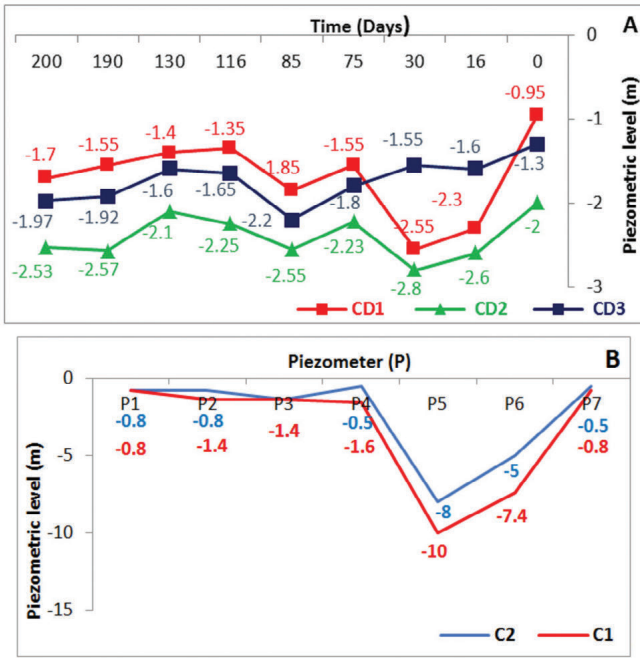


Fig. 10 - Curves of the piezometric level fluctuates in the North of studied area. A) For three core drillings (CD). B) For the piezometers (P) in a specific week in November, where C1 represents the initial piezometric level of the groundwater before rainfall and C2 the groundwater piezometric variation after one week of rainfall.

Fig. 10 - Grafici delle fluttuazioni piezometriche a nord dell'area di studio. A. Per tre sondaggi (CD). B. Nel mese di novembre per i piezometri (P) dove C1 corrisponde al livello iniziale della falda prima delle precipitazioni e C2 all'andamento del livello piezometrico dopo una settimana di precipitazioni.

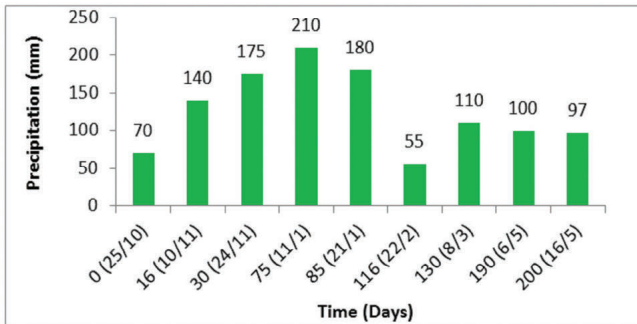


Fig. 11 - Precipitations recorded in the Mila region during the monitoring period.

Fig. 11 - Precipitazioni registrate nella regione di Mila durante il periodo di monitoraggio.

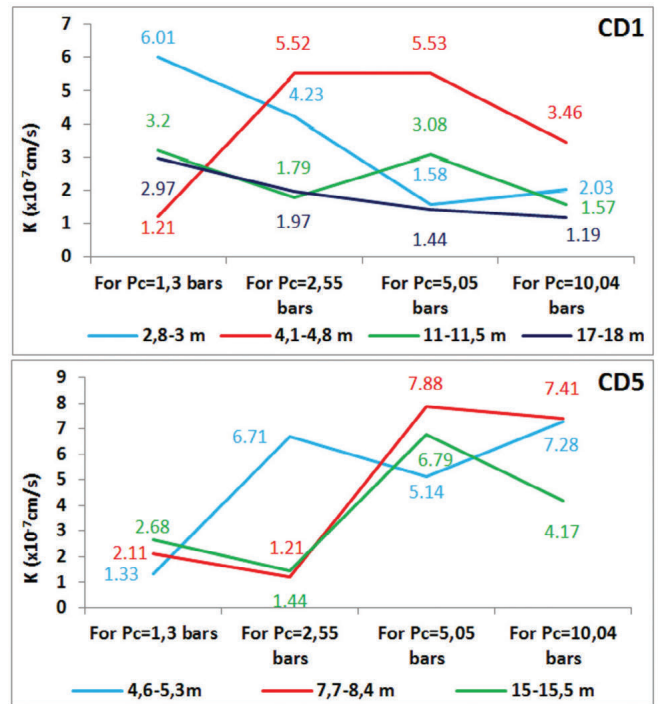


Fig. 12 - Permeability (K) variation curves for some points.

Fig. 12 - Grafici della variazione della permeabilità (K) per alcuni dei punti di indagine.

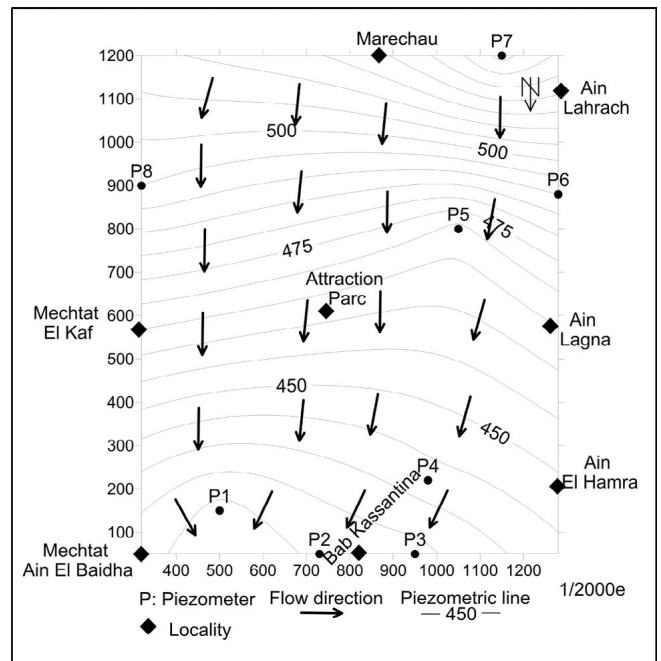


Fig. 13 - Piezometric map of the studied area.

Fig. 13 - Carta piezometrica dell'area di studio.

2.55 bars, 5.05 bars, and 10.04 bars respectively (Fig. 12). The piezometric map establishment of the studied area (Fig. 13) shows that the groundwater flow direction is from the south to north.

Regarding the monitoring of groundwater from shallow wells (CD), the following considerations can be made:

- these wells are drilled into a superficial aquifer with piezometric level from -0.95 to -2.8 m;
- the three wells exhibit the same groundwater behavior: the recharge began after 116 days of rainfall and was followed by a remarkable variation;
- the low permeability of soils leads to low aquifer recharge by infiltration and the high runoff amount, generating the strong alteration of these soils;
- despite the high precipitation amount recorded during 116 days, the piezometric level continues to fall; this means that the aquifer recharge by infiltration is low and indicates the low permeability;
- after the initial 130 days, the piezometric level begins to fall under the effect of the temperature increase and the strong evapotranspiration during the low-flow period.

Regarding the monitoring of piezometers (P), we mark out:

- the piezometers P2, P4, and P7 are in direct relationship to the superficial groundwater, and they are located in places where the infiltrations are considerable which promote their rapid recharge after the rainfall;
- the piezometers P5 and P6 have a deep piezometric level; therefore, they are in relationship to the deep aquifer (karst) and located in places where their recharge is rapid (2 to 2.4 m/week).

These results confirm that the Mila region is characterized by an impermeable soil (weak infiltrations sometimes none), a heavy precipitation from October to May, and superficial flows. Also, it contains two aquifer systems (the first is deep and the second is superficial) (Saadali et al., 2020); their relationship is not excluded through the existing fault network and the deep aquifer system can supply the superficial one.

So, these characteristics have an influence on the soils and their behavior in the studied area where:

- the high precipitations with the absence of vegetal coverage and the low soil permeability (clays), leads to superficial flows; the later favor a high drainage density and the transport of the extracted particles to Mila River causing the contamination and siltation of BeniHaroun dam (Kateb et al., 2020; Habila et al., 2010);
- the steep slope in areas with groundwater flows within and between clay layers, constitutes a trigger factor of landslides and favor the particles pulling, which generating differential settlements; also, the particles are gradually evacuated by flow, in the slope direction (S-N); this phenomenon destabilizes the soil structure and increases the hydraulic gradient locally; if this gradient still increases slightly, the soil lifts; this dangerous phenomenon is related to the speed of water flow; in our case, the provoked hydraulic gradient under

material's nature and hydraulic load, can lead to the infiltration which due to permeability coefficient and infiltration resistance by downward vertical flow; so, it causes cracking and damage to buildings in the studied area (Brencich & Gnecco, 2012; Chettah, 2009; Khellaf, 2019; Hazmoune, 2008);

- the presence of the aquifer in gypsum clay, with limestone blocks and their flows, promote the dissolution of this gypsum which increases the soil aggressiveness for concrete (Khellaf, 2019; Khellaf et al., 2018); furthermore the several landslide seats in our region where the potential of instability risk increases during the winter period (Zouaoui, 2008);
- the presence of groundwater, generally, leads shear resistance reduction (Chen et al., 2019), mechanical characteristic of soils (friction angle ( $\phi$ ), cohesion (C)), and progressive increase deformability under load (Zouaoui, 2008) that influences the bearing soil's capacity (Khellaf, 2019);
- the groundwater fluctuations causing an enormous hydrostatic pressure, recharging/folding, affects the soil volume variation (shrinking-swelling), then the calculation and the proper structural foundations functioning (Khellaf, 2019).

The combination of seismic effect, water presence in soil, strong soil alteration from runoff, and the land slope are considered the destabilizing factors in this region. Consequently, the studied area presents a high risk and its urbanization requires great cautions and all precautions.

## Conclusion

The southeast of the Mila region basin has been selected to expand Mila town, but this area is affected by several natural hazards which require detailed studies. This work aims to characterize the soil in this area through a geotechnical and hydrogeophysical approach.

The geotechnical investigations by the dynamic penetration, core drilling and laboratory tests, have defined the lithology of ground and its characteristics, their resistance and deep of bedrock, for anchoring the foundations.

The hydro-geophysical investigations showed that the most studied layer is a conductive formation, with limestone blocks embedded in it and that the circulation of water in depth within and between layers favors the generation of differential settlements and landslides in the slope direction (S-N).

In relation to the above:

1. the constructions build in this area will certainly undergo displacement in slope direction by the sliding phenomenon and creep, and requires extensive earthworks which will be reactivated the old land movements;
2. the downstream part of the area is marked by several water resurgences indicating significant underground flow. The constructions overload cause an increase in pore pressure and area soil saturation and it causes mudflows.

All the urbanization conditions of the Marechau area, including geological, morphological, geotechnical, and hydrogeological factors, are already unfavorable. Therefore, in the event of any instability phenomena that cannot be controlled, it would be impractical to invest resources in the area. In light of this research it is suggested and recommended that the area be abandoned and another location, which is safer and does not pose any natural hazards, be explored instead. We recommend other detailed studies using geological radar and photo-interpretation and the implementation of a geotechnical map for the Mila region. Furthermore, a continuous survey of landslides (inclinometer monitoring) and groundwater fluctuations (using lot of piezometers) should be necessary. Also, fast vegetation is needed to avoid gully phenomena and to increase the resistance of the soil to shear by the drying of the soil.

#### Acknowledgments

Our sincere thanks go to Sebaai Nedjoua and Bakelli Aissa for their participation in the preparation of this work. The authors are also grateful to the editor as well as the anonymous reviewer for their useful suggestions and constructive comments that improved the quality of this manuscript.

#### Competing interest

On behalf of all authors, the corresponding author states that there is no conflict of interest to disclose.

#### Author contributions

The authors Khoudir KHELLAF, Wahid CHETTAH and Mohamed Amine BECHKIT contributed to the processing of data, writing-original draft preparation, analysis and interpretation of the results.

The author El Hadj YOUCEF BRAHIM contributed to the conception and design of the figures and tables.

The author Imane DIB contributed to the supervision and revising the article critically for important intellectual content; and final approval of the version to be published.

All authors read and approved the final manuscript.

#### Additional information

Supplementary information is available for this paper at <https://doi.org/10.7343/as-2023-630>

Reprint and permission information are available writing to [acquesotterranee@anipapozzi.it](mailto:acquesotterranee@anipapozzi.it)

Publisher's note Associazione Acque Sotterranee remains neutral with regard to jurisdictional claims in published maps and institutional affiliations.

## REFERENCES

- Abbes, K., Dorbath, L., Dorbath, C., Djeddi, M., Ousadou, F., Maouche, S., Benkaci, N., Slimani, A., Larbes, S., & Bouziane, D. (2015). The BeniHaoua, Algeria, Mw 4.9 earthquake: source parameters, engineering, and seismotectonic implications. *Journal of Seismology*, 20(2), 655–667.
- Abbouda, M., Maouche, S., Bouhadad, Y., & Belhai D. (2019). Neotectonics and active tectonics of the Dahra - Lower Chelif Basin (Tell Atlas, Algeria): seismotectonic implication. *Journal of African Earth Sciences*, 153. <http://doi.org/10.1016/j.jafrearsci.2019.02.023>.
- AicheGéo-Sol (Laboratoire d'Études Géotechniques de Sols et Fondations) (2013). Étude géotechnique du POS AU15 sur une surface de 40 ha. Commune de Mila: phase de reconnaissance phase de synthèse III - wilaya de Mila. *Geotechnical study of AU15 POS at 40 ha of surface. Mila Commune: reconnaissance phase, synthesis phase III - Mila wilaya*. File N EG43/12/2013 (in French).
- Alijani-Shirvani, R., & Shooshpasha, I. (2015). Experimental Study on Load-Settlement Behaviour of Cement Stabilised Footing with Different Dimensions on Sandy Soil. *Arab J SciEng*, 40:397–406. <https://doi.org/10.1007/s13369-014-1444-5>.
- Aoudia, A., Vaccari, E., Suhadolc, P., & Meghraoui, M. (2000). Seismogenic potential and earthquake hazard assessment in the Tell Atlas of Algeria. *J. of Seismology*, 4: 79-98.
- Athmania, D. (2010). Minéralogie des argiles et phénomène de retrait-gonflement dans le bassin de Mila (Nord Constantinois). *Mineralogy of clays and shrinkage-swelling phenomenon in the Mila basin (North Constantinois)*. PhD Thesis, University of Constantine, 172 p (in French).
- Ayadi, A., & Bezzeghoud, M. (2015). Seismicity of Algeria from 1365 to 2013: Maximum Observed Intensity Map (MOI 2014). *Seismological Research Letter*, 86 (1). <http://srl.geoscienceworld.org/content/86/1/236.full>.
- Azzouz, F.Z. (2015). Stabilisation des sols argileux de la région de Tlemcen par les sels. *Stabilization of clay soils in the Tlemcen region by salts*. *El Wahat Journal for Research and Studies*, 8 (1): 108-117.
- Beldjoudi, H., Delouis, B., Djellit, H., Yelles-Chaouche, A., Gharbi, S., & Abacha, I. (2016). The Beni-Ilmane (Algeria) seismic sequence of May 2010: seismic sources and stress tensor calculations. *Tectonophysics*, 670:101–114. <https://doi.org/10.1016/j.tecto.2015.12.021>.
- Benabbas, C. (2006). Évolution Mio-Plio-Quaternaire des bassins continentaux de l'Algérie Nord orientale: apport de la photogéologie et analyse morphostructurale. *Mio-Plio-Quaternary evolution of the continental basins of North-Eastern Algeria: contribution of photogeology and morphostructural analysis*. PhD Thesis, University of Constantine (in French).
- Benfedda, A., Serkhane, A., Bouhadad, Y., Slimani, A., Abbouda, M., & Bourenane, H. (2021). The main events of the July–August 2020 Mila (NE Algeria) seismic sequence and the triggered landslides. *Arabian Journal of Geosciences*, 14:1894. <https://doi.org/10.1007/s12517-021-08301-x>.
- Benfedda, A., Abbes, K., Bouziane, D., Bouhadad, Y., Slimani, A., Larbes, S., Haddouche, D., & Bezzeghoud, M. (2017). The August 1st, 2014 (Mw 5.3) Moderate Earthquake: Evidence for an Active Thrust Fault in the Bay of Algiers (Algeria). *Pure Appl. Geophys*, 174: 1503–1511. <https://doi.org/10.1007/s00024-017-1481-6>.
- Benouar, D. (1994). Material for the investigation of the seismicity of Algeria and adjacent regions during the twentieth century. *Annali di geofisica XXXVII*.
- Bouhadad, Y. (2008). Probabilistic seismic hazard assessment in eastern Algeria. *Cahiers du Center Européen de Géodynamique et de Sismologie (ECGS)* 28: 89-94.
- Bounif, A., Haesler, H., & Meghraoui, M. (1987). The Constantine (Northeast Algeria) earthquake of October 27, 1987: surface ruptures and aftershocks study. *Eart.Plan. Sc. Let.* 85: 451-460.



- Brencich, A., & Gnecco, M. (2012). Failure case studies engineering courses and professional practice. *ASCE J.* 37(8); 2113–2126.
- Chanda, D., Saha, R., & Haldar, S. (2019). Influence of Inherent Soil Variability on Seismic Response of Structure Supported on Pile Foundation. *Arabian Journal for Science and Engineering*, 44: 5009-5025. <https://doi.org/10.1007/s13369-018-03699-1>.
- Chen, Y., Li, B., Xu, Y., Zhao, Y., & Xu, J. (2019). Field Study on the Soil Water Characteristics of Shallow Layers on Red Clay Slopes and Its Application in Stability Analysis. *Arabian Journal for Science and Engineering*, 44: 5107-5116. <https://doi.org/10.1007/s13369-018-03716-3>.
- Chettah, W. (2009). Investigation des propriétés minéralogiques et géomécaniques des terrains en mouvement dans la ville de Mila « Nord-Est d'Algérie ». *Investigation of the mineralogical and geomechanical properties of moving terrain in the city of Mila « Northeast of Algeria »*. Magister memory, El Hadj Lakhdar-Batna University (in French).
- Coiffait, P. E. (1992). Un bassin post-nappe dans son cadre structural, exemple du bassin de Constantine (Algérie orientale). *A post-groundwater basin in its structural framework, example of the Constantine basin (Eastern Algeria)*. PhD thesis in science. Université de Nancy (in French).
- Cordary, D. (1994). Mécanique des sols. *Mechanic of soils*. Lavoisier ed. Tec and Doc. Paris (in French).
- Costet, J., & Sanglerat, G. (1981). Cours pratique de mécanique des sols. Tome 1 - Plasticité et calcul des tassements. *Practical course in mechanics of soils. Volume 1 - Plasticity and settlement calculation*. Dunod ed. Paris (in French).
- Dakshanamurthy, V., & Raman, V. (1973). A simple method of identifying an expansive soil. *Soils and Foundations*. Japanese Soc. Of Soil Mech. And Foundation Eng, 13(1): 97-104.
- Derriche, Z., Guechtal, L., & Tas, M. (1999). Comportement des ouvrages dans les argiles expansives d'In-Aménas. *Behavior of structures in expansive clays of In-Aminas*. French Geotechnical Journal, 86: 55-63 (in French).
- Durand-Delga, M. (1955). Etude géologique de l'Ouest de la chaîne Numidique. *Western geological survey of the Numidic chain*. PhD thesis, Paris. Publ. Serv. Carte Géol. Algérie, 2e Sér, Bull. 24 (in French).
- El Yakoubi, N. (2006). Potentialités d'utilisation des argiles marocaines dans l'industrie céramique: cas des gisements de Jbel Kharrou et de Benhmed (Meseta marocaine occidentale). *Potential uses of Moroccan clay in the ceramic industry: case of the Jbel Kharrou and Benhmed deposits (western Moroccan meseta)*. PhD thesis, Mohammed V-Agdal University, Rabat Faculty of Science (in French).
- Géoeexplo (Bureau d'étude géophysique et exploration). (2015). Etude des glissements de terrain dans la wilaya de Mila par approche géophysique. *Study of landslides in the wilaya of Mila by geophysical approach* (in French).
- Habila, S., Khelili, S., & Legouchi, E. (2010). Assessment of the risk of contamination of the waters of the Beni Haroun Dam (Wilaya de Mila) by organic pollutants and minerals. "International Network Environmental Management Conflicts, Santa Catarina R Brasil", 1(1), pp. 239-245 (in French).
- Hadji, R., Rais, K., Gadri, L., Chouabi, A., & Hamed, Y. (2016). Slope Failure Characteristics and Slope Movement Susceptibility Assessment Using GIS in a Medium Scale: A Case Study from Ouled Driss and Machroha Municipalities, Northeast Algeria. *Arab J Sci Eng*, 42: 281-300. DOI 10.1007/s13369-016-2046-1.
- Hamidatou, M., & Sbartai, B. (2015). Probabilistic seismic hazard assessment in the Constantine region, Northeast of Algeria. *Arab J Geosci*, 10:156. <https://doi.org/10.1007/s12517-017-2876-5>.
- Harbi, A., Maouche, S., & Ayadi, A. (1999). Neotectonics and associated seismicity in the Eastern Tellean Atlas of Algeria. *J. Seismol*, 3: 95-104.
- Harbi, A., Meghraoui, M., & Maouche, S. (2011). The Djidjelli (Algeria) earthquakes of 21 and 22 August 1856 (Io=VIII, IX) and related tsunami effects. *Reviaread. J Seismol*, 15(1):105-129.
- Hazmoune, H. (2008). Approches des études géotechniques liées à la pathologie des ouvrages: étude de cas des 185 logements de Mila. *Approches to geotechnical studies related to the pathology of structures: case study of 185 dwellings in Mila*. Magister memory, University of Constantine, 86 p (in French).
- Kateb, Z., Bouchelkia, H., Benmansour, A., & Belarbi, F. (2020). Sediment transport modeling by the SWAT model using two scenarios in the watershed of Beni Haroun dam in Algeria. *Arab J Geosci* 13, (653):1-17. <https://doi.org/10.1007/s12517-020-05623-0>.
- Khellaf, K., & Bitat, F. (2006). Etude géotechnique et géologique des 185 logements (Mila) et proposition de solutions aux problèmes posés. *Geotechnical and geological study of 185 dwellings (Mila) and proposal of solutions to the problems raised*. Engineer memory, Jijel University (in French).
- Khellaf, K. (2009). Cadre géologique, aspect pétro-minéralogique et géotechnique du complexe argilo-marneux de la région Nord-Ouest de la ville de Mila: Boufouh (Mila-Algérie (Nord orientale). "Geological, petro-mineralogical and geotechnical aspect of the clay-marl complex of the North-West region of the city of Mila: Boufouh (Mila-Algérie (North-East)". Magister Memory, Cheikh Larbi Tébessi-Tébessa University, 156p (in French).
- Khellaf, K., Zeroual, F., Sebaai, N., & Aziz, W. (2015). L'effet de l'ajout du sable de Sidi Abd el Aziz (Jijel) sur le potentiel du gonflement des argiles de Mila (région d'el kherba). *The effect of the addition of the sand of Sidi Abd el Aziz (Jijel) on the potential swelling of the Mila clay (El Kherba region)*. El Wahat for Research and Studies, 8(2): 57 – 77 (in French).
- Khellaf, K., & Hamimed, M. (2018a). Contribution to the geotechnical study and estimation for differential settlements of Mila region soils (North-East Algeria). *JARST* 5(2): 818-828.
- Khellaf, K., & Hamimed, M. (2018b). Petro-Mineralogical and Geotechnical Analysis on the Clays of Constantinois Province (Mila North-East Algeria). *J. Appl. Environ. Biol. Sci*, 8(2):14-22.
- Khellaf, K., & Hamimed, M. (2018c). Geotechnical study and estimation for differential settlements risk of Mila-Constantine basin soils (north-east Algeria). *El Wahat pour les Recherches et les Etudes*, 11(1): 109-126.
- Khellaf, K. (2019). Cadre géologique, minéralogique et analyses des différents paramètres des formations argileuses variées en zone occidentale du bassin de Mila, Algérie Nord orientale. *Geological, mineralogical framework and analyses of the various parameters of the various clay formations in the western zone of the Mila basin, Algeria North East*. PhD thesis, University of Tebessi, Tebessa (in French).
- Kherroubi, A., Deverchère, D., Yelles, A., Mercier de Lepinay, B., Domzig, A., Cattaneo, A., Bracene, R., Gaullier, V., & Graindorge, D. (2009). Recent and active deformation pattern off the easternmost Algerian margin, western Mediterranean sea: New evidence of contractional tectonic reactivation. *Marine Geology*, 261: 17-32.
- Komornik, A., & David, D. (1969). Prediction of swelling pressure of clays. *Journal of Soil Mechanics and Foundation Engineering Division ASCE*, 95 (1): 209-225.
- Labioud, F. (2009). Mouvement de masses et instabilités des terrains dans le bassin versant de l'oued Mila. Caractérisations et enjeux socio-économiques. *Mass movement and land instability in the Wadi Mila watershed. Characterizations and socio-economic issues*. Magister memory, University of Science and Technology – Houari Boumediene- Algiers (in French).
- LBM-Sol (Laboratoire de Béton et de Mécanique de Sol). (2014). Rapport d'étude géotechnique: Plan d'occupation de sol N°9 Mil. (2ème et 3ème phase). *Geotechnical Study Report: Land Use Plan 9 Mil. (2nd and 3rd phase)*. File 32/2012 (in French).

- LNHC (Laboratoire Nationale de l'Habitat et de Construction). (2001). Rapport d'étude géotechnique complète du POS de Mila. *Comprehensive geotechnical study report of the Mila POS*. File 133/2001. OPGI de Mila (in French).
- Loke, M.H., & Barker, R.D. (1995). Least-square deconvolution of apparent resistivity pseudo-sections. *Geophysics* 60(6):499-523.
- Maouche, S., Meghraoui, M., Morhange, C., Belabbes, S., Bouhadad, Y., & Haddoum, H. (2011). Active coastal thrusting and folding, and uplift rate of the Sahel Anticline and Zemmouri earthquake area (Tell Atlas, Algeria). *Tectonophysics*, 509: 69-80. <https://doi.org/10.1016/j.tecto.2011.06.003>.
- Mebarki, A. (1984). Ressources en eau et aménagement en Algérie. Le bassin du Kébir Rhumel. *Springs and development in Algeria. The Kébir Rhumel basin*. University Publication Office Ed. 8, Algiers (in French).
- Mebarki, A., & Thomas, C. (1988). Analyse des relations entre écoulements superficiels et souterrains à partir des hydrogrammes des cours d'eau: application au bassin du Kebir-rhumel dans le Constantinois (Algérie). *Analysis of the relationships between surface and underground flows from river hydrographs: application to the Kebir-rhumel basin in Constantinois (Algeria)*. *Continental Hydrology*, 3(2), 89-103. ISSN 0246-1528 (in French).
- Meghraoui, M. (1988). Géologie des zones sismiques du Nord de l'Algérie. *Paléosismologie, tectonique active et synthèse sismotectonique. Geology of seismic zones in northern Algeria*. Paleoseismology, active tectonics and seismotectonic synthesis. PhD thesis, Univ. Paris VI (in French).
- Mutlutürk, M., & Balcioglu, E. (2015). Geo-Engineering Properties and Swelling Potential of Quaternary Lacustrine Clays in North of Burdur, Turkey. *Arabian Journal for Science and Engineering* 40: 1917-1931. <https://doi.org/10.1007/s13369-014-1505-9>.
- NF P18-011. (1992). Sols: Reconnaissance et Essais: Classification des environnements agressifs. *Soils: Recognition and Testing: Classification of Aggressive Environments*. Certified June, Bull, lab link. P. and Ch (in French).
- NF P94-050. (1994). Sols - Reconnaissance et Essais: Détermination de la teneur en eau pondérale des sols - Méthode par étuvage. *Soils - Recognition and Testing: Determination of water-weight content of soils - Steaming method*. Registered October 1991. Bull, liaison labo. P. and Ch. 190 (in French).
- NF P94-053. (1994). Sols - Reconnaissance et Essais: Détermination de la masse volumique des sols fins en laboratoire - Méthode de la trousse coupante, du moule et de l'immersion dans l'eau. *Soils - Recognition and Testing: Determination of the density of fine soils in the laboratory - Method of cutting kit, mould and immersion in water*. Approved October 1991. Bull, lab liaison. P. and Ch (in French).
- NF P94-057. (1994). Sols - Reconnaissance et Essais: Analyse granulométrique des sols par sédimentation. *Soils - Recognition and Testing: Particle size analysis of soils by sedimentation*. Approved May 1992. Bull, lab link. P. and Ch (in French).
- NF P94-090-1. (1997). Sols: Reconnaissance et Essais - Essai œdométrique - Partie 1: Essai de compressibilité sur matériaux fins quasi saturés avec chargement par paliers. *Soils: Recognition and Testing - Oedometer Testing - Part 1: Compressibility Testing on Near-Saturated Fine Materials with Step Loading* 55p (in French).
- Parker, W. L. (1977). Understanding inverse theory. *Ann Rev Earth Planet Sci*. 1977: 5: 35-64.
- Philipponnat, G. (1979). Fondations et ouvrages en Terre. *Foundations and Earth structures*. Eyrolles ed. (Paris) (in French).
- Philipponnat, G., & Hubert, B. (2003). Fondations et ouvrages en terre. *Foundations and Earth structures*. Eyrolles ed. (Paris) (in French).
- Rollings, R.S., Burkes, J. P., & Rollings, M. P. (1999). Sulfate Attack on Cement-Stabilized Sand. *Journal of Geotechnical and Geoenvironmental Engineering*, 125(5): 364-372.
- Saadali, B., Khedidja, A., Mihoubi, N., Ouddah, A., Djebassi, T., & Kouba, Y. (2020). Water quality assessment and organic pollution identification of Hammam-Grouz dam (Northeastern Algeria). *Arabian Journal of Geosciences*, 13 (20), 1091.
- Suiki, S. (2007). Les argiles du bassin de Constantine-Mila: composition minéralogique, chimique et répartition des gisements. *The clays of the Constantine-Mila basin: mineralogical, chemical composition and distribution of deposits*. Magister memory, Univ. Constantine, 129 pp (in French).
- Tebbouche, M. Y., Ait Benamar, D., Hany, M. H., Singh, A.P., Bencharif, R., Machane, D., Aghiles Meziani, A., & Nemer, Z. (2022). Characterization of El Kherba landslide triggered by the August 07, 2020, Mw =4.9 Mila earthquake (Algeria) based on post event field observations and ambient noise analysis. *Environmental Earth Sciences*, 81:46. <https://doi.org/10.1007/s12665-022-10172-8>.
- Touati, F. (2019). Étude géophysique, géologique, géotechnique de l'aléa naturel du glissement de terre cas de commune (Ain Tinn) wilaya de Mila. *Geophysical, geological, geotechnical study of the natural hazard of the landslide: case of Ain Tine commune, wilaya de Mila*. Magister memory, Ferhat Abbas Sétif University 1, 96p (in French).
- Vila, J. M. (1980). La chaîne alpine d'Algérie orientale et des confins algéro-tunisiens. *The Alpine chain of Eastern Algeria and the Algerian-Tunisian borders*. PhD thesis, Paris VI2 (in French).
- Zouaoui, S. (2008). Étude géologique et géotechnique des glissements de terrains dans le bassin néogène de Mila: glissement de Sibari. *Geological and geotechnical study of landslides in the Mila Neogene Basin: Sibari Landslide*. Magister memory, El Hadj Lakhdar- Batna University (in French).